

A Simple Global Resonance Strategy for Wideband Discrete-Time MASH $\Sigma\Delta$ Modulators

Beheshte Khazaeili and Mohammad Yavari

Integrated Circuits Design Laboratory, Department of Electrical Engineering,
Amirkabir University of Technology
Tehran, Iran

Emails: b.khazaeeli@aut.ac.ir, myavari@aut.ac.ir

Abstract— A novel strategy of zero optimization in cascaded $\Sigma\Delta$ modulators is presented. In the proposed structure, by using just an analog inter-stage feedback path, one pair of the noise transfer function (NTF) zeros is distributed over the desired bandwidth so that the in-band quantization noise is reduced. The effectiveness of the proposed modulator is verified by analytical calculations and simulation results.

Keywords— MASH $\Sigma\Delta$ modulators; zero optimization; local resonance; global resonance;

I. INTRODUCTION

High speed $\Sigma\Delta$ A/D converters are widely used in both emerging wired and wireless communications systems [1]. An appropriate structure for wideband applications with low oversampling ratios (OSRs) is multi-stage noise-shaping (MASH) modulators which enable high-order noise shaping without any stability problems. To get higher resolutions, the zero optimization is a good technique to reduce the in-band quantization noise without increasing the number of integrators. To do this, the local resonance strategy can be used [2, 3]. Using this strategy for MASH $\Sigma\Delta$ modulators ($\Sigma\Delta$ Ms) may affect the digital filters. So, their implementation becomes complicated [4]. Another zero optimization approach called the global resonance has been presented in [1, 4] for a MASH 2-2 modulator. In this technique, the zero optimization is done by using inter-stage feedback paths so that the digital filters in the conventional MASH modulator do not change. Consequently, in some cases, the global resonance can be a better choice for MASH $\Sigma\Delta$ Ms.

In this paper, a simple approach is presented to optimize one pair of overall noise transfer function (NTF) zeros in a typical discrete-time MASH $\Sigma\Delta$ modulator. This is done just by using an extra analog inter-stage feedback path. Thus, with a minimal extra circuit, the zero optimization can be done for a conventional MASH $\Sigma\Delta$ modulator without affecting the digital filters.

II. CONVENTIONAL MASH $\Sigma\Delta$ MODULATOR

As is known, in a conventional 2-stage MASH $\Sigma\Delta$ modulator, the first-stage quantization noise is used as the input to the second stage. Ideally, by assuming high accuracy analog circuits, the first-stage quantization error is cancelled by the following digital signal processing logic. Thus, in the output of the overall modulator, just the input signal and the shaped

quantization error of the second stage modulator are appeared. The shaping order of this quantization noise is equal to the order of the overall cascaded $\Sigma\Delta$ modulator [5].

III. PROPOSED MASH $\Sigma\Delta$ MODULATOR

The block diagram of the proposed MASH $\Sigma\Delta$ modulator is shown in Fig. 1. In this structure, the first-stage quantization noise is fed to the second stage similar to the conventional 2-stage MASH modulator. The last non-delaying integrator of the first-stage is separated from the rest of the loop filter. In the second stage, a unity signal transfer function (STF) $\Sigma\Delta$ modulator is used where the first delaying integrator is taken apart from the other of the loop filter.

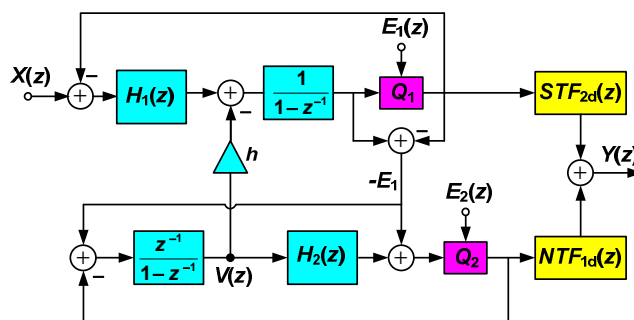


Fig. 1. Block diagram of the proposed MASH $\Sigma\Delta$ modulator.

By using a unity STF structure in the second stage of the proposed MASH modulator, the analog circuit requirements become more relaxed [6]. Moreover, the first integrator output of this stage is given by:

$$V(z) = -\frac{z^{-1}}{1-z^{-1}} NTF_2(z)E_2(z) \quad (1)$$

where NTF_i and E_i denote the NTF and quantization noise of the i -th stage, respectively. $NTF_1(z)$ and $NTF_2(z)$ depend on the loop filters of the first and second stages, respectively, and are given by:

$$NTF_1(z) = \frac{1}{1+H_1(z) \times 1/(1-z^{-1})} \quad (2)$$

$$NTF_2(z) = \frac{1}{1+H_2(z) \times z^{-1}/(1-z^{-1})} \quad (3)$$

A ratio of $V(z)$ is injected to the input of the last non-delaying integrator in the first stage. The overall output of the modulator shown in Fig. 1 is as follows:

$$\begin{aligned}
Y(z) &= STF_1(z)STF_{2d}(z)X(z) \\
&+ [NTF_1(z)STF_{2d}(z) - STF_2(z)NTF_{1d}(z)]E_1(z) \\
&+ \left[NTF_{1d}(z)NTF_2(z) - h \times V(z) \times \frac{1}{1-z^{-1}} NTF_1(z)STF_{2d}(z) \right] E_2(z)
\end{aligned} \quad (4)$$

where STF_i denotes the signal transfer function of the i -th stage. NTF_{id} and STF_{id} are the digital estimates of NTF_i and STF_i , respectively. By assuming a perfect matching between the analog and digital filters and $STF_2(z) = 1$, by substituting (1) for $V(z)$ in (4), the modulator's output will be as:

$$\begin{aligned}
Y(z) &= STF_1(z)X(z) \\
&+ \frac{NTF_1(z)NTF_2(z)[1 - (2-h)z^{-1} + z^{-2}]}{(1-z^{-1})^2} E_2(z)
\end{aligned} \quad (5)$$

As it is seen from (5), the quantization error of the first-stage is cancelled like the conventional MASH modulator. By choosing a proper value for coefficient h , one pair of NTF zeros can be optimized without any need to change the digital cancellation filters. Indeed, two dc zeros of the overall NTF are cancelled and instead two optimized zeros are placed inside the desirable bandwidth. Note that the places of these zeros are the function of coefficient h and depend on OSR. The lower OSR results in the higher optimal value of h which is easier to realize. Thus, the proposed strategy is more suitable for wideband applications with low values of OSR. The optimal value of h can be computed by $h = 2 - 2\cos(2\pi f_0/f_s)$ where f_s is the sampling frequency. Optimal place of optimized NTF zeros is given by $f_0 = \sqrt{(2L-3)/(2L-1)}f_{BW}$ where L and f_{BW} denote the modulator's order and signal bandwidth, respectively [2].

The proposed modulator structure has another advantage over the traditional MASH modulator. Since the second stage quantization error is uncorrelated to all other signals in the first stage, it operates as a dither signal there.

For the above-mentioned advantages, the proposed modulator needs just one simple extra analog inter-stage feedback path that is shown by the path with coefficient h in Fig. 1.

As a case study, consider we need a fourth-order noise-shaping. To achieve this, different structures of MASH modulators like the MASH 2-2 or MASH 3-1 can be chosen. In next sections, these two structures using the proposed and conventional zero optimization strategies are compared.

A. MASH 2-2 Modulator

MASH 2-2 modulator based on the proposed structure is shown in Fig. 2. In this figure, d and d_{Dig} denote the inter-stage gain and its digital estimation, respectively. Assuming $d_{Dig}=d$, the ideal output of the proposed MASH 2-2 modulator is as follows:

$$Y(z) = X(z) + \frac{1}{d} \left(1 - z^{-1}\right)^2 \left[1 - (2-h)z^{-1} + z^{-2}\right] E_2(z) \quad (6)$$

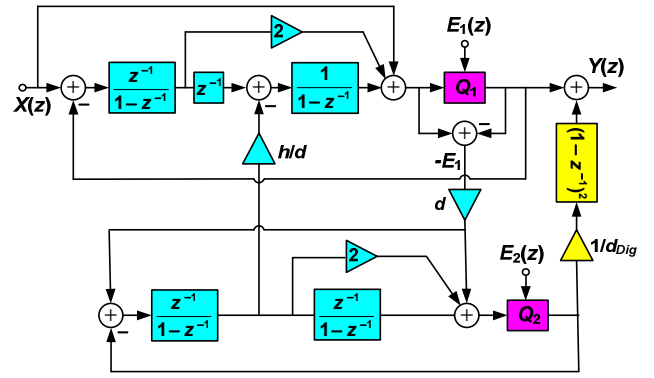


Fig. 2. Proposed MASH 2-2 $\Sigma\Delta$ modulator.

To optimize the NTF zeros in a MASH 2-2 modulator, the local and global resonance strategies are shown in Fig. 3 and Fig. 5 in [1], respectively. The proposed MASH 2-2 is compared with these two structures:

The proposed modulator needs just one analog coefficient (h) to make the resonance instead of three coefficients ($(2-k)$, $(1-k)$, k) in the modulator with local resonance presented in [1]. This makes the modulator realization simpler and decreases the sensitivity to circuit non-idealities. The price to pay is one extra digital-to-analog converter (DAC) to extract the first-stage quantization noise.

The proposed MASH 2-2 modulator has two advantages over the global resonance-based modulator shown in Fig. 5 in [1]. Firstly, the proposed structure needs just one extra inter-stage feedback path instead of two in [1]. Secondly, the destination of the two inter-stage feedback paths in [1] is the input of the first-stage quantizer whereas in the proposed MASH 2-2 modulator, one inter-stage feedback path enters the last non-delaying integrator of the first-stage. Thus, the passive implementation of the adder before the first-stage quantizer becomes simpler (the adder needed before the quantizer in a unity STF structure, can be implemented either with a passive or an active circuit as presented in [6]).

B. MASH 3-1 Modulator

To the best of the authors' knowledge, the only strategy already used to optimize one pair of NTF zeros in a MASH 3-1 modulator is the local resonance. This strategy is compared with the proposed approach. Fig. 3 shows the conventional MASH 3-1 modulator with the local resonance. The modulator used in the first-stage is based on the structure presented in [2]. As is known, to eliminate the first-stage quantization noise in the overall output of the modulator, the second-stage digital filter has to be equal to the first-stage NTF. So, it has a pair of complex conjugate zeros which is difficult to implement efficiently. Also, the appearance of β in this digital filter makes the modulator to be sensitive to the mismatch between the analog β and its digital estimation.

The MASH 3-1 modulator based on the proposed structure is shown in Fig. 4. Thanks to the using of global resonance, the second-stage digital filter is the same as in the conventional MASH 3-1 with no resonance. So, it is easy to implement and also independent of the coefficient h . Consequently, the

sensitivity mentioned for the modulator shown in Fig. 3, is cancelled in the proposed MASH 3-1 modulator.

Equation (6) is also established for the ideal output of the modulators shown in Fig. 3 and Fig. 4.

C. Comparison of MASH 3-1 and MASH 2-2 Modulators

In a real circuit, the first-stage quantization noise leaks to the overall output of the modulator while it is attenuated by a noise-shaping function with the same order as the first-stage modulator. So using higher order modulators in the first-stage of the cascaded $\Sigma\Delta$ s, makes the circuit requirements more relaxed. The cost to pay is that the input signal amplitude is reduced.

As an example, the relation (7) shows the first-stage quantization noise leakage to the overall output of a typical MASH $\Sigma\Delta$ modulator, due to the mismatch between the analog inter-stage gain d and its digital estimation, d_{Dig} . To achieve this equation, it is assumed that all analog transfer functions are well-matched to their digital estimations.

$$\begin{aligned}
 Y(z) &= STF_1(z)STF_2(z)X(z) \\
 &+ NTF_1(z)STF_2(z)\left(1 - d / d_{Dig}\right)E_1(z) \\
 &+ NTF_1(z)NTF_2(z)E_2(z)
 \end{aligned} \quad (7)$$

As is seen, $E_1(z)$ is shaped by the first-stage NTF. So, it can be concluded that MASH 3-1 modulator is less sensitive to the mismatch between d and d_{Dig} , compared to the MASH 2-2 modulator. So, considering the above-mentioned advantages of MASH 3-1 over the MASH 2-2 as well as the simple realization of the proposed structure, the proposed MASH 3-1 performs better than MASH 2-2 with global resonance shown in Fig. 5 in [1]. The truth of above-mentioned subjects will be shown by simulation results in the next section.

IV. SIMULATION RESULTS

The proposed MASH 3-1 $\Sigma\Delta$ modulator shown in Fig. 4 along with the conventional MASH 3-1 with no resonance and MASH 2-2 modulator with global resonance shown in Fig. 5 in [1] were simulated using MATLAB and Simulink. Effects of some circuit non-idealities including the limited swing and finite dc gain of the amplifiers were considered in Simulink using the models proposed in [7]. The number of quantization bits in both stages was 4. The sampling frequency of 160 MHz was used. The OSR was 8 and a -4 dBFS sinusoidal input signal was used in the simulations. The inter-stage gain, d , was assumed to be 2.

Fig. 5 shows the simulated output spectrum of the proposed MASH 3-1 with optimal value of $h=0.1$ and the conventional MASH 3-1 modulator with no resonance. As is seen, using the proposed strategy makes a notch near to the band limit. The achieved signal-to-noise and distortion ratio (SNDR) is 89.8 dB and 78.9 dB for the proposed MASH 3-1 modulator and conventional MASH 3-1 modulator with no resonance, respectively. So, by using the proposed strategy, SNDR is improved about 10.9 dB compared to the conventional MASH 3-1 with no resonance.

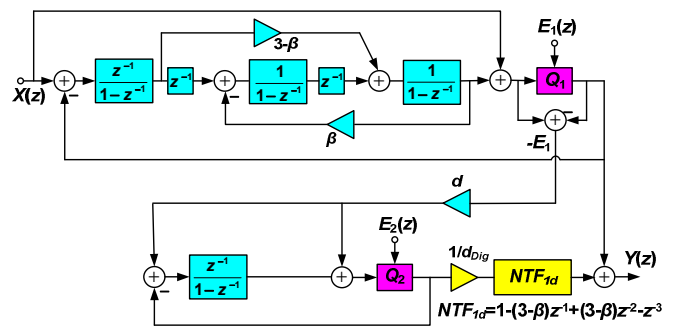


Fig. 3. Conventional MASH 3-1 modulator with local resonance.

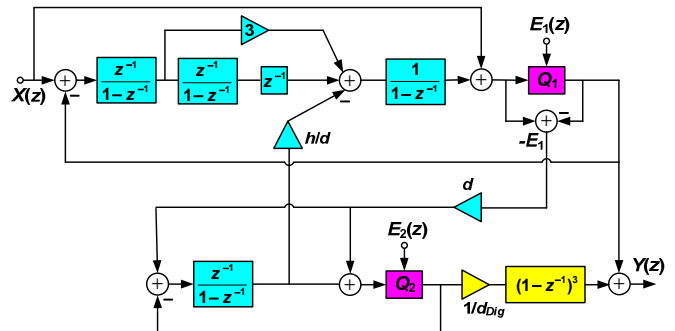


Fig. 4. Proposed MASH 3-1 modulator.

The simulated SNDR versus the input signal amplitude is shown in Fig. 6. As is seen, the proposed MASH 3-1 has an overload level factor about 0.7 dB lower than the conventional MASH 3-1 with no resonance. The reason is that the first-stage quantizer of the proposed MASH 3-1, must also process a ratio of the second-stage quantization error. So, in comparison to the conventional MASH 3-1, the input signal with lower amplitude can overload it. Although this condition is also instated for the MASH 2-2 with global resonance presented in [1] with respect to the conventional MASH 2-2 modulator, but its overload level factor is about 2.1 dB higher than the proposed MASH 3-1 modulator. This is the result of using lower order modulator in the first stage.

The simulated SNDR versus the first integrator amplifier DC gain is plotted in Fig. 7. As is seen the minimum DC gains of 45 dB and 56 dB are required to prevent the SNDR degradation of the proposed MASH 3-1 and global resonance-based MASH 2-2 modulators, respectively. Thus, the first integrator amplifier in the proposed MASH 3-1 modulator needs 11 dB lower DC gain compared to the MASH 2-2 with global resonance presented in [1]. So, the power consumption is reduced.

SNDR variations due to the mismatch between d and d_{Dig} so that $d=d_{Dig}(1-\delta_d)$, is illustrated in Fig. 8. As theoretically was expected, the proposed MASH 3-1 modulator is less sensitive to this mismatch compared to the MASH 2-2 with global resonance presented in [1].

Fig. 9 shows the SNDR variations due to the non-ideal capacitor ratios which make resonance coefficients β and h in MASH 3-1 modulators shown in Fig. 3 and Fig. 4. Assume $\beta = \beta_{ideal}(1 - \delta_\beta)$ and $h = h_{ideal}(1 - \delta_h)$ where h_{ideal} and β_{ideal} denote the ideal value of h and β . As was indicated in section B, the digital filter independency from h in the proposed modulator makes it to be insensitive to this mismatch.

V. CONCLUSION

A novel topology of discrete-time MASH $\Sigma\Delta$ modulators with optimized NTF zeros has been presented. One pair of NTF zeros is optimized just by using one extra simple analog inter-stage path. The proposed strategy does not depend on the modulator order and is a suitable choice for wideband and low voltage applications.

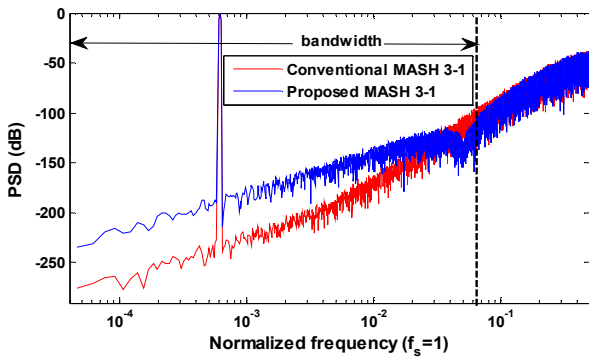


Fig. 5. Simulated output spectrum.

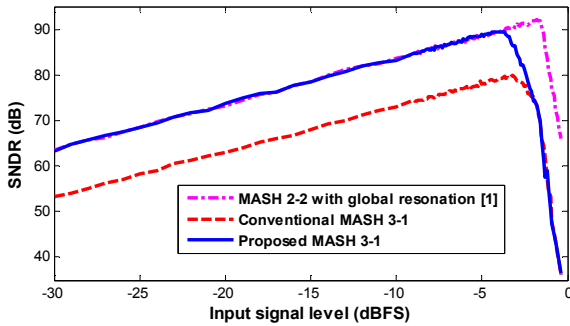


Fig. 6. SNDR versus the input signal amplitude.

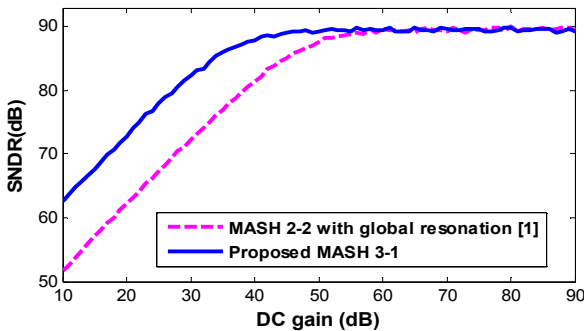


Fig. 7. SNDR versus the first amplifier DC gain.

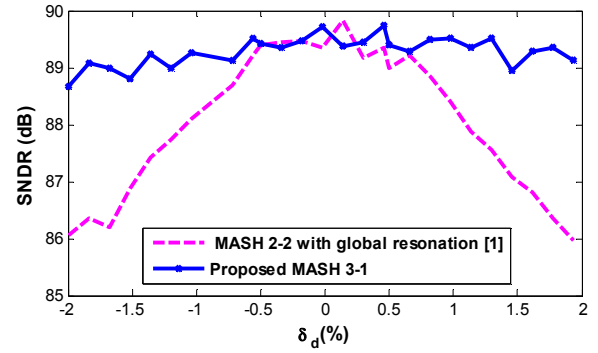


Fig. 8. SNDR degradation versus mismatch between the analog inter-stage gain d and its digital estimate d_{dig} .

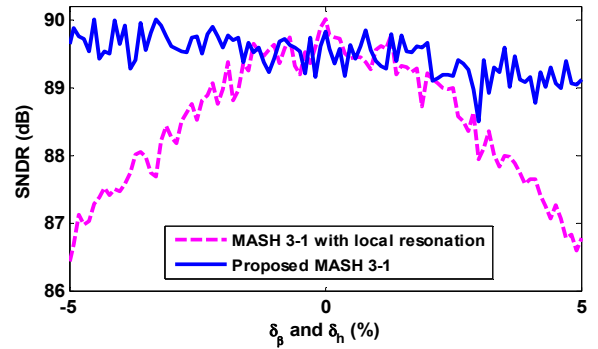


Fig. 9. SNDR variations versus mismatch between the ideal and real values of h and β .

REFERENCES

- [1] A. Morgado, R. del Río, and J. M. de la Rosa, "Two novel cascade $\Sigma\Delta$ modulator for broadband low-voltage A/D conversion," in *Proc. IEEE MWSCAS*, pp. 478-481, Aug. 2008.
- [2] A. Hamoui and K. Martin, "High-order multibit modulators and pseudo data weighted-averaging in low oversampling $\Sigma\Delta$ ADCs for broadband applications," *IEEE Trans. Circuits Syst.-I*, vol. 51, no. 1, pp. 72-85, Jan. 2004.
- [3] Y. Du, T. He, Y. Jiang, S. Sin, S. U. R. P. Martins, "A robust NTF zero optimization technique for both low and high OSRs sigma-delta modulators," in *Proc. IEEE APCCAS*, pp. 29-32, Dec. 2012.
- [4] M. Sanchez-Renedo, S. Paton, and L. Hernandez, "A 2-2 discrete time cascaded $\Sigma\Delta$ modulator with NTF zero using interstage feedback," in *Proc. Int. Conf. on Electronics, Circuits and Systems*, pp. 954-957, Dec. 2006.
- [5] R. Schreier and G.C. Temes, *Understanding delta-sigma data converters*, IEEE Press/Wiley, Piscataway, NJ, pp. 127-136, 2005.
- [6] Z. Sohrabi and M. Yavari, "A 13 bit 10 MHz bandwidth MASH 3-2 $\Sigma\Delta$ modulator in 90 nm CMOS," *Int. Journal of Circuit Theory and Applications*, vol. 41, no. 11, pp. 1136-1153, Apr. 2012.
- [7] P. Malcovati, S. Brigati, F. Francesconi, F. Maloberti, P. Cusinato, and A. Baschiroto, "Behavioral modeling of switched-capacitor sigma-delta modulators," *IEEE Trans. Circuits Syst.-I*, vol. 50, no. 3, pp. 352-363, Mar. 2003.